Supplemental material

Construction and stereotactic injection of vectors for LH3 knockdown and overexpression

For local knockdown of LH3 *in vivo*, recombinant AAV (type 9) vectors expressing a short hairpin RNA (shRNA) directed at the LH3 (AAV-shLH3) or a control hairpin (AAV-shCon) were used (GeneChem, Shanghai, China). The shRNA expression is driven by a mouse U6 promoter (pol III) and use GFP as a reporter. The final virus in PBS had a titer of 3×10^{12} viral particles/ml. To induce exogenous expression of LH3 *in vivo*, we constructed pAAV9-LH3-p2A-GFP vector (AAV-LH3) by inserting mouse LH3 cDNA into pAAV9-p2A-GFP between two ITRs (ViGene Biosciences, Shandong, China). Adeno-associated viral carrying GFP (AAV-GFP) was simultaneously prepared as a control. Mice were anesthetized with 2% isoflurane, consisting of an O_2 mixture (1L/min). Then mice were fixed in the stereotaxic frame with mouse adaptor (World Precision Instruments, FL, USA) to place the skull horizontally. We stereotaxically placed the tip of the needle (10microL syringe Model 701 with 26g 2inch Hamilton Replacement needle Point, Fisher Scientific, USA) at both sides of the ventricles using the coordinate obtained from Mouse Brain Atlas (0.2 mm caudal and 0.9 mm lateral to bregma, and 3.0 mm ventral to the skull surface). A total volume of 10μl of supernatant containing 3×10^{10} AAV-shLH3 or AAV-shCon viral particles was injected by ultramicropump (World Precision Instruments, FL, USA) at 0.2 μL/min. Similarly, a total volume of 2μl of supernatant containing 2×10^{11} AAV-LH3 or AAV-GFP viral particles was injected at 0.2 μL/min. After finishing the injection, the needle was held still for 15 minutes before withdrawal. The bone hole was sealed with bone wax and the wound was stitched.

RNA sequencing

Total RNA was purified by RNeasy micro kit (QIAGEN, Hilden, Germany). The TruSeq RNA Sample Preparation Kit V2 (Illumina, San Diego, CA) was used for next generation sequencing library construction per manufacturer's protocols. The cDNA product was amplified, and sequencing adapters and barcodes were ligated onto the fragments for each respective sample to create cDNA libraries ready for sequencing. The sequencing was performed by Shanghai Biotechnology Corporation (Shanghai, China) using the Illumina high-throughput HiSeq 2500 platform.

The cleaning sequencing data without ribosome RNA reads for each sample were aligned to reference genome.[1] Then, four procedures 'stringtie, stringtie --merge, cuffquant, cuffnorm'[2-4] with default parameters were used to reconstruct transcripts, identify novel transcripts, quantify transcripts and normalize expression values (FPKM, Fragments per Kilobase of transcript per Million mapped reads). For differential expression analysis, the R language (v3.2.1) with edgeR package was used to identify the differential expression genes (DEGs).[5] The fold change between the two groups was calculated as: logFC=log2 (Experimental/Control group). Gene in two groups, whose $|logFC| > 1$ and q-value < 0.05, was defined as DEGs in this study. DEGs hierarchically clustered to represent the expression patterns by using ward method for euclidean distance matrix. Clustered gene expression profile was showed with the mean of $\log_2$(FPKM) in each group. The software of interproscan (v.5.8-49.0) and blast2go were used to annotate the domains, gene families and gene ontology (GO) functions. The KOBAS (v2.0)[6] was used to mapping the genes to KEGG pathways with default parameters. A hyper geometric distribution test was carried out to identify GO functions and KEGG pathways in which DEGs were significantly

enriched (q-value < 0.05), comparing to total background expressed genes. Enriched GO items and KEGG pathways were plotted by python (v.2.7.5) with matplotlib (v.1.4.3) package. The gene-functional network was reconstructed in Cytoscape (v.3.6.0).

Sequencing data have been uploaded to the National Center for Biotechnology Information with the GEO accession number GSE113151 and are publically available.

Isolation of cerebral vessels

Brains were collected for the isolation of cerebral vessels as previously described.[7, 8] During this period, mice did not develop any neurologic signs. Briefly, mice were transcardially perfused with ice-cold PBS. Then, the brains were removed, rinsed in cold isotonic sucrose buffer (0.32 mol/L sucrose, 3 mmol/L HEPES, pH 7.4), and cleared of pia mater and choroid plexus. The brain was homogenized with a tight-fitting pestle Dounce homogenizer in 5 ml of sucrose buffer. The homogenate was centrifuged at 1000 g for 10 min. The supernatant containing neuronal cells was discarded, and the white layer of myelin in the upper part of the pellet was removed. The pellet was resuspended in 5 ml of the same cold buffer and centrifuged at 1000 g for another 10 min. We repeated the washes three times to eliminate the rest of the myelin and free neurons. The pellet was resuspended in 3 ml of the sucrose buffer and centrifuged at 350 g to eliminate detached cells. This step was repeated three times, and the resulting pellet was resuspended in 1 ml of sucrose buffer and centrifuged at 75 g for 5 min. The resulting supernatant was used as the cerebral vessel preparation.

Supplemental Figures

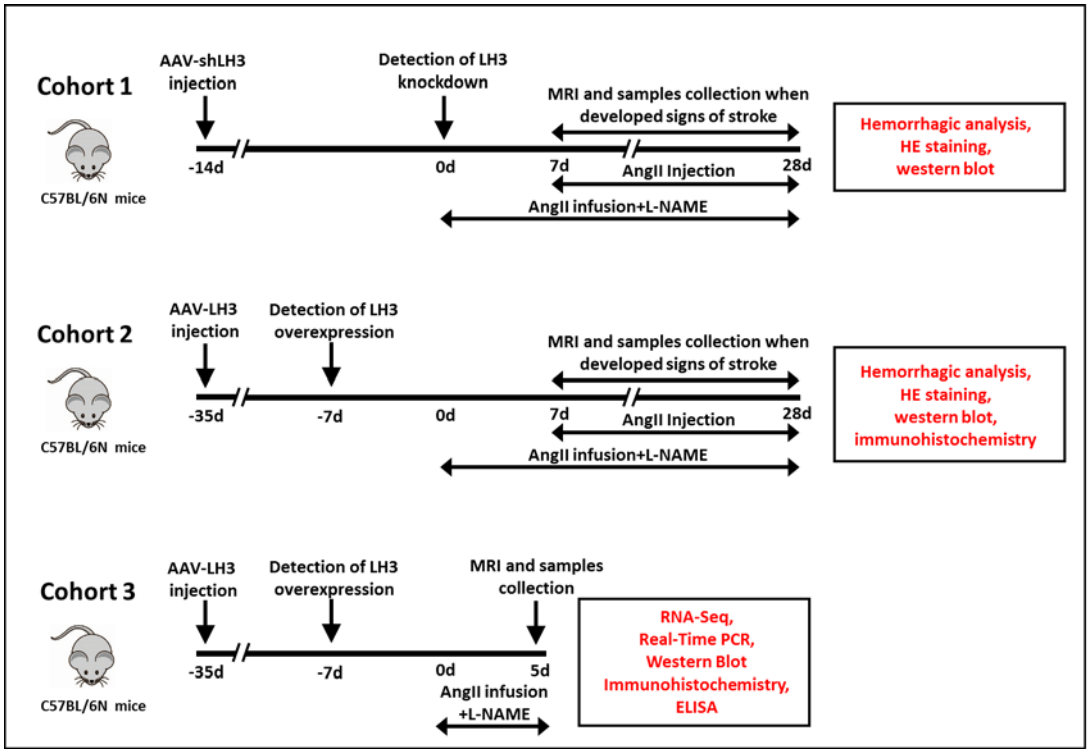

Supplemental Figure 1. Schematic diagram illustrates the drug administration and experimental design of 3 cohorts of mice.

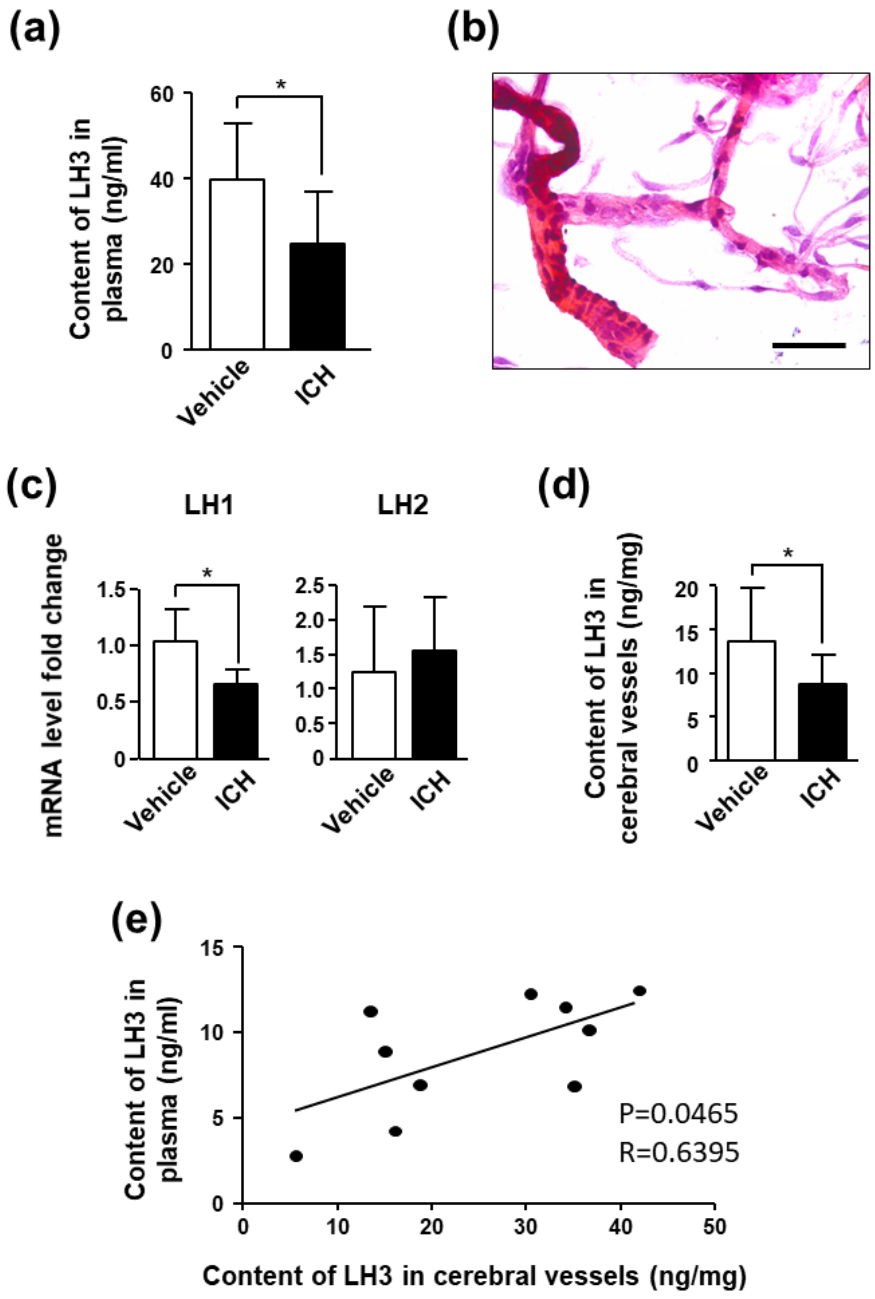

Supplemental Figure 2. Changes in LH3 levels in plasma and cerebral vessels of mice after intracerebral hemorrhage (ICH) **(a).** The concentrations of LH3 in plasma were measured by ELISA. n=10. **P*<0.05; Student's unpaired two-tailed t-test. **(b).** Representative image of isolated cerebral vessels for subsequent experiments stained by hematoxylin and eosin (H&E). **(c).** Quantitative PCR was used to evaluate the expression of mRNA levels of LH1 and LH2 isoenzymes in cerebral vessels after ICH

in mice. n=6. *P<0.05; Student's unpaired two-tailed t-test. **(d).** The concentrations of LH3 in cerebral vessels were measured by ELISA. n=10. *P<0.05; Student's unpaired two-tailed t-test. **(e).** The correlation of LH3 levels between plasma and cerebral vessels. n=10. The Pearson correlation test. Bar = 50 μm. Data are mean±SD.

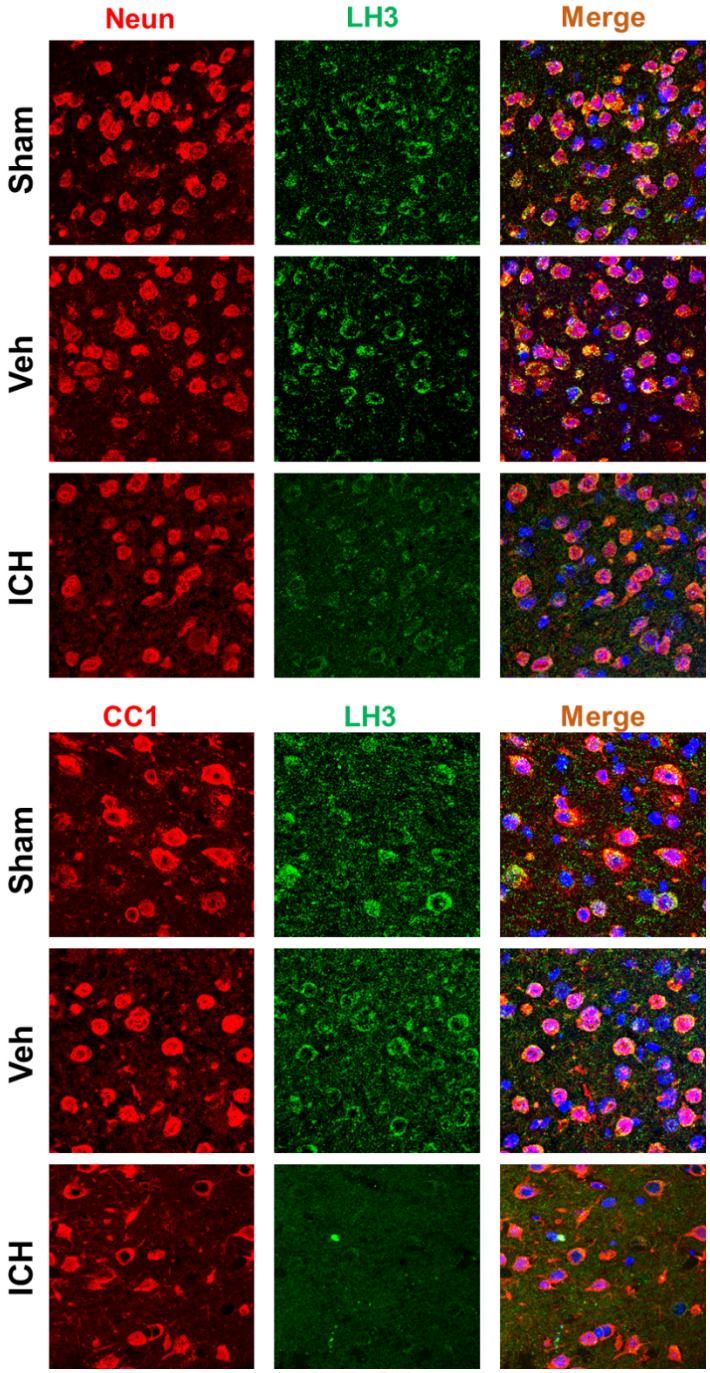

Supplemental Figure 3. Detection of LH3 in neurons and oligodendrocytes after

intracerebral hemorrhage (ICH). Representative images of LH3 expression on $NeuN^+$ neurons **(a)** and $CC1^+$ oligodendrocytes **(b)** in the mice of the sham, vehicle (Veh) and ICH groups. Bar = 50 μm.

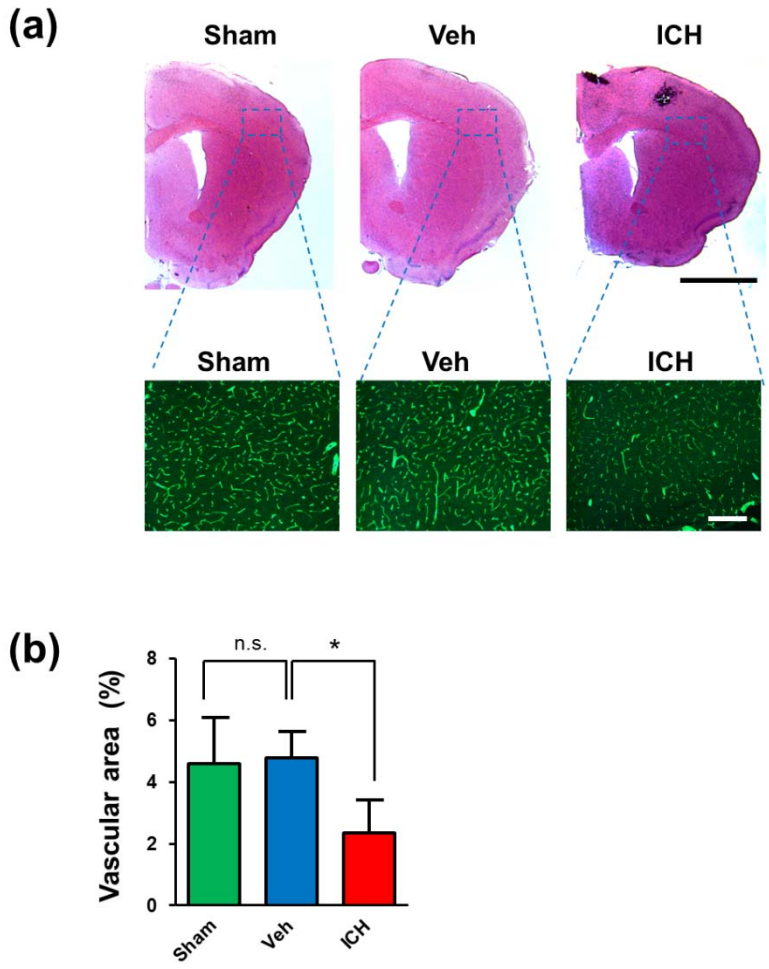

Supplemental Figure 4. Detection of $CD31^+$ cerebral vessels in brain after intracerebral hemorrhage (ICH). (a) Representative images of section of brain were staining with hematoxylin and eosin (H&E) **(upper panel**, bar = 2 mm**)**, and $CD31^+$ cerebral vessels were observed in the cortex region **(lower panel**, bar = 200 μm**)**. (b) Quantification of percent area occupied by $CD31^+$ vascular structures for each group. Data are mean±SD. n=6. *P<0.05, n.s. indicates not significant; one-way ANOVA with Bonferroni post hoc test.

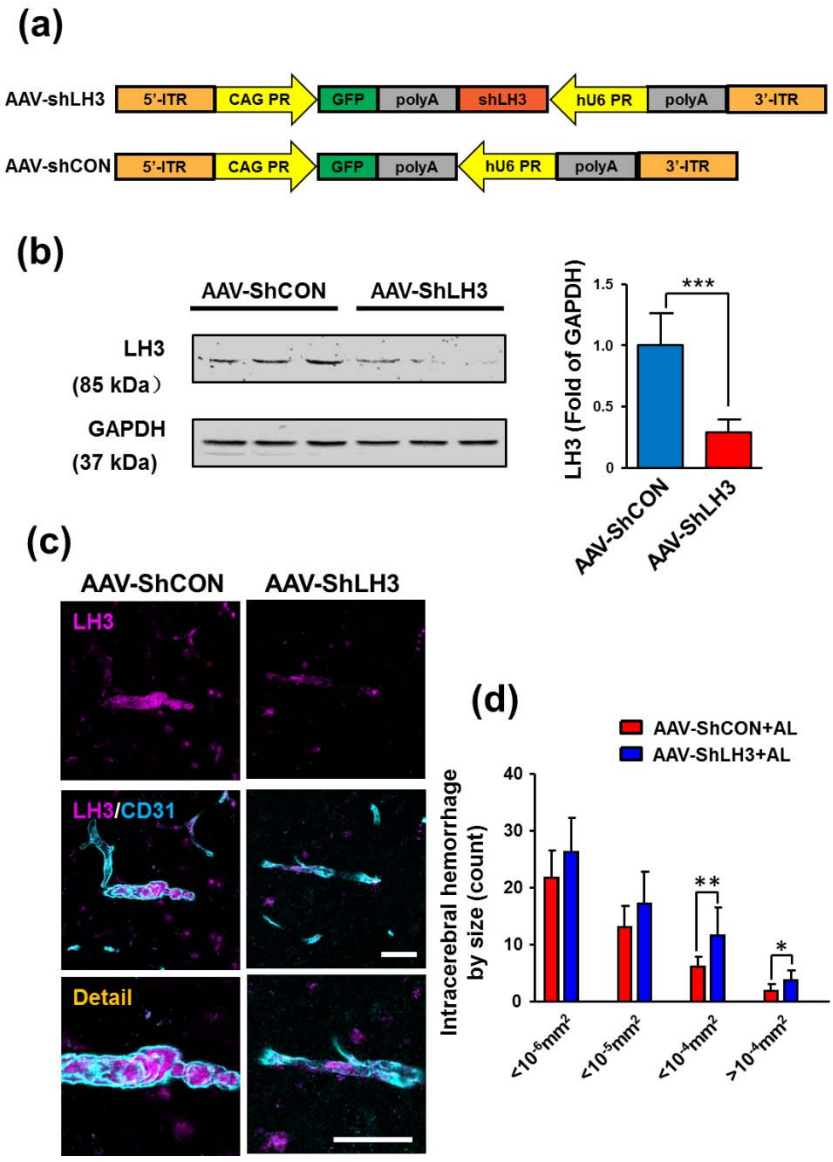

Supplemental Figure 5. Examination of LH3 knockdown in mouse brains *in vivo*. **(a).** The structures of shRNA-containing vector. **(b).** Western blot analysis of LH3 in the cerebral vessels 2 weeks after AAV-shLH3 or AAV-shCon delivery into the mouse brain. n=6. ***P<0.001; Student's unpaired two-tailed t-test. **(c).** Representative images of LH3 expression on $CD31^+$ cerebral vessels in each group. **(d).** Quantification of the distribution of ICH by size in shCON+AL mice (n=14) and

shLH3+AL mice (n=18). Bar = 25 μm. n=6. *P<0.05, **P<0.01; Student's unpaired two-tailed t-test. Data are the mean±SD.

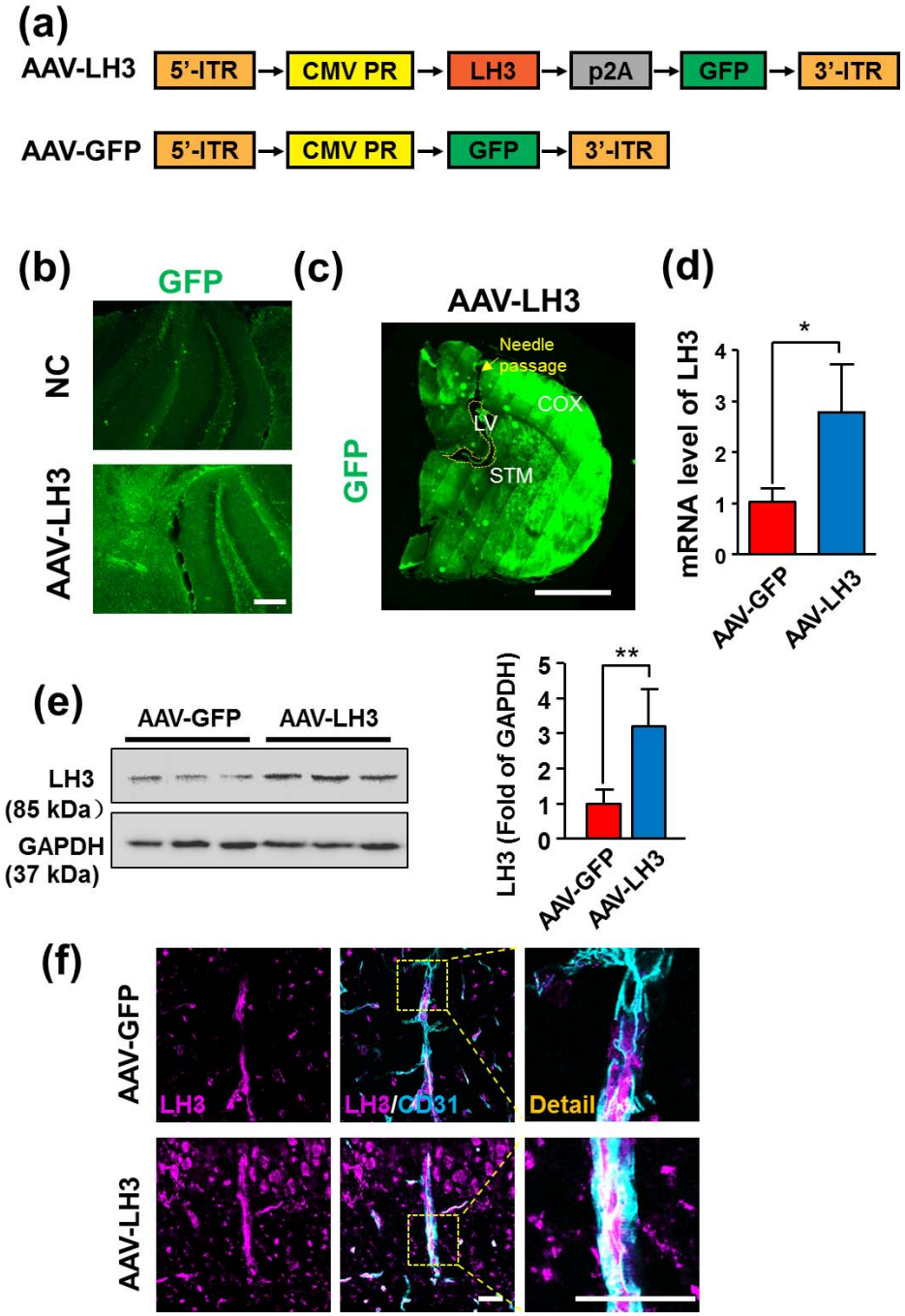

Supplemental Figure 6. Examination of LH3 overexpression in mouse brains *in vivo*. **(a).** AAV vector structures. Schematic diagram showing that LH3 cDNA was sub-cloned between two ITRs in *pAAV9-LH3-p2A-GFP vector.* **(b).** GFP fluorescence

(green) **s**howed AAV-LH3 expression *in vivo* at 4weeks after stereotaxic delivery into the mouse brain. Bar = 200 μm. **(c).** Representative images of GFP fluorescence (green) acquired by a whole-slide imaging system. Bar = 2 mm. **(d).** Quantitative PCR was used to evaluate the expression of mRNA levels of LH3 at 4weeks after AAV-LH3 or AAV-GFP delivery into the mouse brain. n=6. **P*<0.05; Student's unpaired two-tailed t-test. **(e).** Western blot analysis of LH3 in the cerebral vessels 4 weeks after AAV-LH3 or AAV-GFP delivery into the mouse brain. n=6. ***P*<0.01; Student's unpaired two-tailed t-test. **(f).** Representative images of LH3 expression on $CD31^+$ cerebral vessels in each group. Bar = 200 μm. COX, cortex. STM, striatum. LV, lateral ventricle. Data are mean±SD.

Supplemental Figure 7. Elevated systolic blood pressure of mice subjected to AngII plus L-NAME. Systolic blood pressure in each group subjected to AngII plus L-NAME (AL), evaluated 7 days after initiation of hypertension. Data are mean±SD. n=15. ***P<0.001; two-way ANOVA with Bonferroni post hoc test.

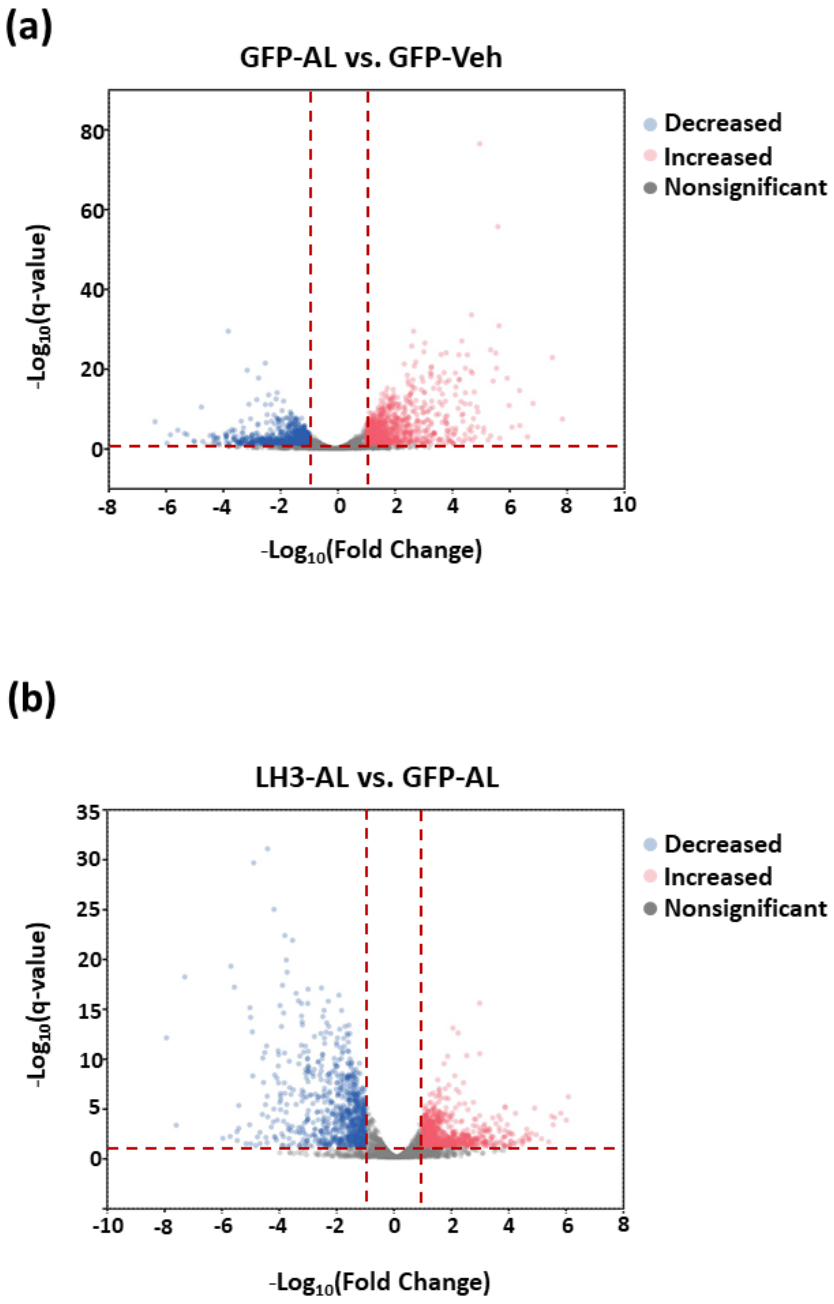

Supplemental Figure 8. Overview of the differential expression genes (DEGs) in cerebral vessels of mice after treatment. Volcano plot displaying DEGs in cerebral vessels of mice were shown: **(a)** at day 5 after subjected to vehicle or AngII plus L-NAME (AL) in AAV-GFP treated groups, **(b)** between AAV-GFP and AAV-LH3 treated groups at day 5 after subjected to AL. The x axis represents $-\log_{10}$ (fold difference between two groups); the y axis represents $-\log_{10}$ (q-value). Each spot represents a gene.

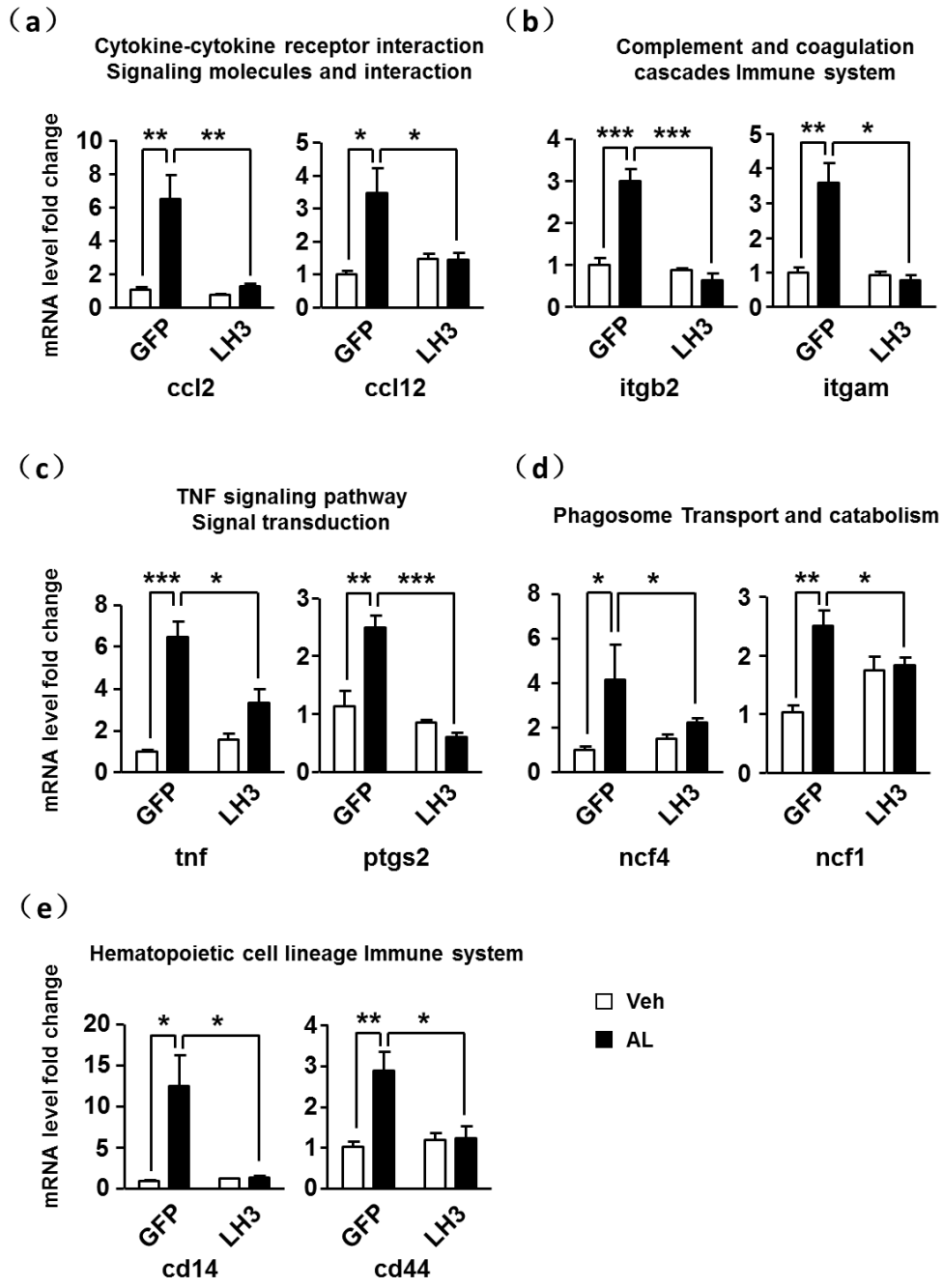

Supplemental Figure 9. Validation of pivotal genes enriched in the top 5 signaling pathways by RNA-seq. Quantitative PCR was used to evaluate the expression of pivotal genes that was significantly reversed by the overexpression of LH3. Data are mean±SD. n=6. **P*<0.05, ***P*<0.01, ****P*<0.001; two-way ANOVA with Bonferroni post hoc test or a Kruskal–Wallis ANOVA combined with Dunn's post hoc multiple comparison test.

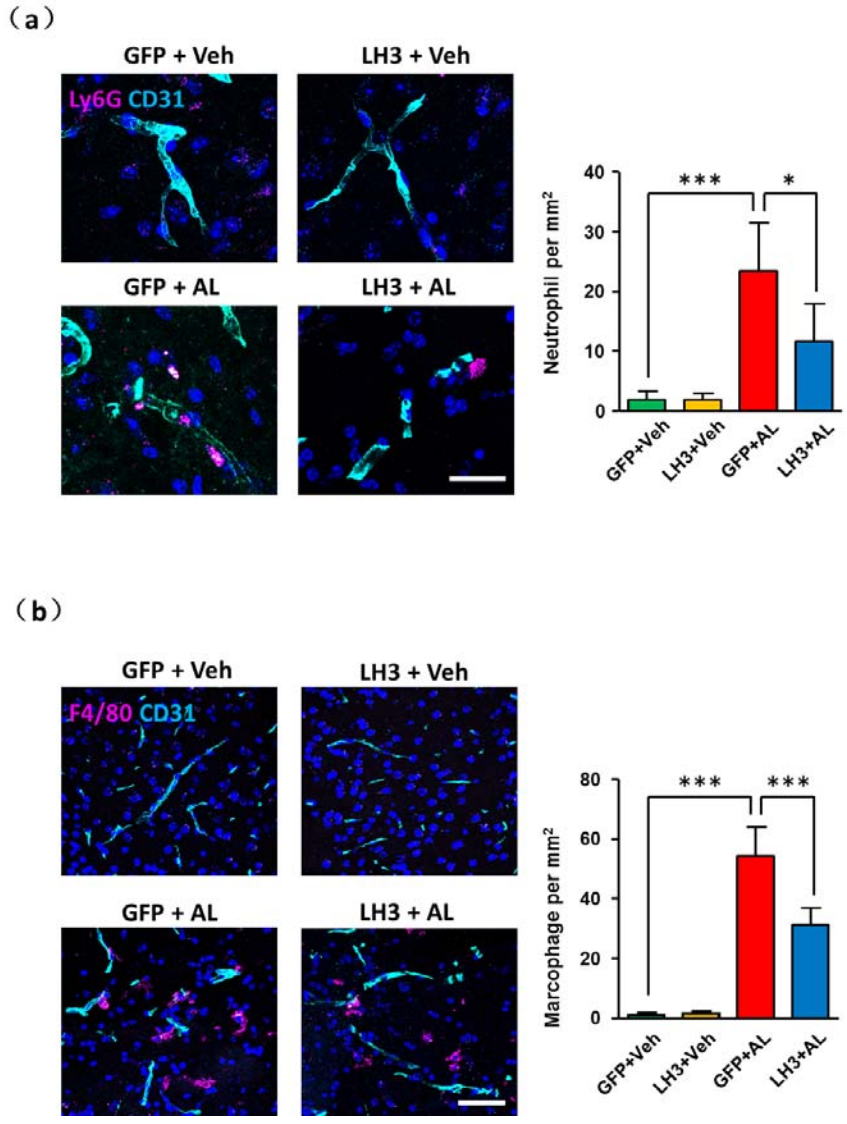

Supplemental Figure 10. Infiltration of neutrophil and macrophage into perivascular spaces were ameliorated by LH3 overexpression. Representative images and quantification of Ly-6G$^+$ neutrophil **(a)** and F4/80$^+$ macrophage **(b)** immunostaining surrounding CD31$^+$ cerebral vessels at day 5 after subjected to AngII plus L-NAME (AL) in AAV-GFP and AAV-LH3 treated mice. Bar = 50 μm. n=6, **P*<0.05, ****P*<0.001; two-way ANOVA with Bonferroni post hoc test.

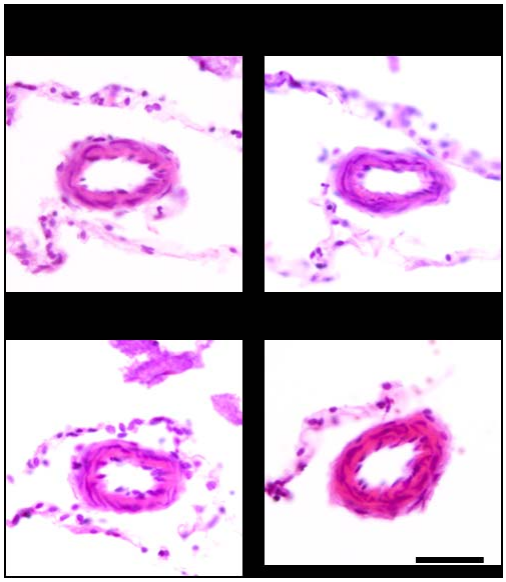

Supplemental Figure 11. LH3 overexpression maintained the hypertrophic wall thickness of cerebral small arteries. Representative images of cerebral small arteries stained by hematoxylin and eosin (H&E) at day 5 after subjected to AngII plus L-NAME (AL) in AAV-GFP and AAV-LH3 treated mice. Bar = 50 μm.

References

1. Kim D, Langmead B, Salzberg SL. HISAT: a fast spliced aligner with low memory requirements. *Nat Methods* 2015; 12: 357-360.

2. Kim D, Pertea G, Trapnell C, et al. TopHat2: accurate alignment of transcriptomes in the presence of insertions, deletions and gene fusions. *Genome Biol* 2013; 14: R36.
3. Pertea M, Pertea G. M, Antonescu CM, et al. StringTie enables improved reconstruction of a transcriptome from RNA-seq reads. *Nat Biotechnol* 2015; 33: 290-295.
4. Trapnell C, Roberts A, Goff L, et al. Differential gene and transcript expression analysis of RNA-seq experiments with TopHat and Cufflinks. *Nat Protoc* 2012; 7: 562-578.
5. Nikolayeva O, Robinson MD. edgeR for differential RNA-seq and ChIP-seq analysis: an application to stem cell biology. *Methods Mol Biol* 2014; 1150: 45-79.
6. Xie C, Mao X, Huang J, et al. KOBAS 2.0: a web server for annotation and identification of enriched pathways and diseases. *Nucleic Acids Res* 2011; 39: W316-W322.
7. Yamakawa H, Jezova M, Ando H, et al. Normalization of endothelial and inducible nitric oxide synthase expression in brain microvessels of spontaneously hypertensive rats by angiotensin II AT1 receptor inhibition. *J Cereb Blood Flow Metab* 2003; 23: 371-380.
8. Bengrine A, Da SC, Massy ZA, et al. Cerebral arterioles preparation and PECAM-1 expression in C57BL/6J and ApoE-/- mice. *Front Biosci (Landmark Ed)* 2011; 16: 2367-2371.